JOURNAL OF GUIDANCE, CONTROL, AND DYNAMICS
Vol. 25, No. 3, May–June 2002

Phugoid Damping Control

Meir Pachter* and Nicolas J. Schindeler†
Air Force Institute of Technology, Wright–Patterson Air Force Base, Ohio 45433

A novel phugoid damping control design methodology is developed, based on the use of wind axes and a point-mass aircraft model. The state variables are air speed, flight-path angle, and heading angle; the control variables are thrust setting, angle of attack, bank angle, and sideslip angle; and the command signals are air speed, flight-path angle, and heading angle or heading rate. All of the variables and parameters are nondimensionalized. A multivariable set point controller is developed that consists of the following: First, it consists of a trim calculation-based nonlinear feedforward control computer; thus, given a commanded new trim state (air speed, flight-path angle, and yaw rate), the required trim thrust setting and trim angle of attack, bank angle, and sideslip angle inputs are determined. Second, the controller consists of a small signal linear feedback regulator. The equations of motion linearized about the trim condition of wings level and constant altitude flight, which simplify the dynamics to allow separation between the lateral and longitudinal control channels, are used, and a small-signal linear multivariable regulator is designed. The linear compensator also entails integral action. Thus, the controller consists of a strongly nonlinear feedforward module and a linear small-signal compensator. The novel proposed multivariable and nonlinear set point controller encompasses full three-axes autopilot functions. Moreover, this controller is used as a tracking controller, also known as a phugoid damping controller, provided that the bandwidth of the command signal is substantially less than the bandwidth of the closed-loop flight control system. The phugoid damping controller's performance is examined in extensive simulations, and its wide operational envelope is demonstrated.

Nomenclature

AR	=	aspect ratio
a_T	=	tail lift curve slope
a_W	=	wing lift curve slope
b	=	wing span
C_D	=	drag coefficient
C_{D0}	=	zero-lift drag coefficient
C_L	=	lift coefficient
D	=	drag
e	=	error signal
F	=	side force
f_s	=	sampling frequency
g	=	acceleration of gravity
K	=	parabolic drag polar constant
K_I	=	controller gain matrix, integral part
K_P	=	controller gain matrix, proportional part
$K_{\cdot,\cdot}$	=	controller gain
L	=	lift
m	=	mass
$\bar{q}$	=	dynamic pressure
S_T	=	vertical tail surface area
S_W	=	wing surface area
T	=	thrust
t	=	time
t_s	=	settling time
V	=	velocity
z	=	integrator charge
α	=	angle of attack
β	=	sideslip angle
γ	=	flight-path angle
μ	=	thrust (normalized)
ξ	=	phugoid damping ratio
ξ_L	=	lateral control channel's damping ratio (specified)
ξ_P	=	longitudinal control channel's damping ratio (specified)
ρ	=	air density
τ	=	directional control channel's time constant (specified)
ϕ	=	bank angle
ϕ_D	=	disturbance bank angle
ψ	=	heading angle
ω_n	=	phugoid natural frequency
ω_{n_L}	=	lateral control channel's natural frequency (specified)
ω_{n_P}	=	longitudinal control channel's natural frequency (specified)
$\bar{\omega}$	=	yaw rate at trim

Received 4 May 2001; revision received 30 July 2001; accepted for publication 29 October 2001.

*Professor, Department of Electrical and Computer Engineering.
†Student, Department of Electrical and Computer Engineering.

I. Introduction

PHUGOID damping control entails the design of compensators for the control of the aircraft's slow states. Thus, in the pitch channel, one controls the air speed and flight-path angle. In the directional channel, the heading angle is controlled. When one's attention is confined to the regulation function, one then refers to autopilots, namely, altitude-hold, Mach-hold, and heading-hold autopilots. Traditionally, automatic pilots have been used extensively in missiles and in aircraft to decrease pilot workload and improve flight safety. It is envisioned that, in the future, complex outer-loop flight control systems will be used increasingly in the control of emerging uninhabited combat air vehicles (UCAVs). Thus, the challenge is to increase the operational envelope that autopilots can successfully handle and also to increase the bandwidth of the command signals that outer-loop tracking controllers, also known as phugoid damping controllers, can successfully handle, thus endowing UCAVs with high-performance autonomous flight control systems.

Model-based control design is standard practice in aerospace. Conventional autopilot design, as espoused, for example, in Ref. 1, is almost exclusively based on a linear plant model derived from a linearization of the six-degree of freedom aircraft equations of motion. One acknowledges the inherently slow timescale of the autopilot controlled variables by using a nested control loop structure. The inner loops consist of the stability augmentation system (SAS) and control augmentation system (CAS), whereas the autopilot is relegated to the outer loop. Typically, control loops for aircraft control systems are designed from the inside out. That is, the first step is the design of an inner-loop SAS, where the actuator dynamics are also accounted for. From there, the design moves progressively to the outer loops: CAS and altitude-/Mach-/heading–hold autopilots. Moreover, the standard autopilot is a linear compensator, augmented

with gain scheduling.[2] Conventional autopilots have performed well over many decades. At the same time, the operational envelope of conventional autopilots is somewhat limited, namely, the linear control design envisages small perturbations in the states, low-amplitude set point changes, and slowly varying set point settings. Thus, in World War II, the autopilot controlled V1 cruise missile was downed by Royal Air Force (RAF) pilots by exploiting the V1 autopilot's limited operational envelope: They tipped the V1s over with their wingtips.[3,4] Also, autopilot upsets have been reported in recent times.[5,6]

In the present paper, the model-based design of the autopilot/outer-loop controller hinges on a low-order point-mass model of the aircraft dynamics. The low-order dynamics exclusively encompass the states relevant to autopilot design. The fast inner-loop states are the control variables. The novel approach to outer-loop controller design pursued in this paper is as follows: Directly design the outer-loop controller employing a low-order, slow-dynamics, albeit nonlinear, model. It is hypothesized that such an approach would simplify the outer-loop controller design and help better capture the nonlinear characteristics of the air vehicle. The latter is, in part, conducive to a full envelope controller, thus obviating the need for gain scheduling. Although this approach does not include the fast inner-loop state dynamics in the outer-loop controller's design, and one relies on a robust inner-loop controller,[7] ensuring that the outer-loop controller yields sufficient phase margin to compensate for this deficiency. We believe that ab initio use of a low-order plant model is the right approach to outer-loop controller/autopilot design. Moreover, by use of the right plant model, a trim solution-based nonlinear controller naturally suggests itself. Hence, a high-quality outer-loop nonlinear controller/autopilot with an expanded operational envelope is realized.

Specifically, in this paper, a novel phugoid damping control design method is developed, based on the use of wind axes and a low-order point-mass aircraft model. The state variables are air speed, flight-path angle, and heading angle; the control variables are thrust setting, angle of attack, bank angle, and sideslip angle; and the command (reference) signals are air speed, flight-path angle, and heading angle or heading rate. All variables and parameters are nondimensionalized. A multivariable set point controller is developed that consists of the following: First, it consists of trim calculation-based nonlinear feedforward control computer; thus, given a commanded new trim state (air speed, flight path angle, and yaw rate), the required trim thrust setting, angle of attack, roll angle, and sideslip angle inputs are determined. Second, the controller consists of a small-signal linear feedback multivariable regulator. The equations of motion are linearized about the trim condition of wings level, constant altitude flight, which simplifies the dynamics to allow separation between the lateral and longitudinal control channels. The linear compensator also entails integral action. Thus, the controller consists of a strongly nonlinear feedforward module and a linear small-signal multivariable tracking controller. The novel proposed multivariable set point controller encompasses full three-axes autopilot functions. Moreover, this controller is used as a tracking controller, provided that the bandwidth of the command signal is substantially less than the bandwidth of the closed-loop flight control system, and we then refer to the phugoid damping controller. It is envisaged that the latter will receive inputs from a higher-level supervisory control module, thus affording UCAVs a high degree of control autonomy.

The paper is organized as follows. In Sec. II, the aircraft model is introduced. The aircraft parameters are representative of an F-16 class aircraft flying at 200 m/s at 20,000 ft and are given in Table 1. Section II also introduces the wind axes used in the design, the nondimensionalized equations of motion, and the aircraft trim control settings required to achieve a commanded trim state. In Sec. III, the linearized equations of motion are derived. These linearized equations of motion and, in particular, the trim condition of wings level, constant altitude flight, with trim speed equal to initial speed, simplify the dynamics and allow decoupling between the lateral and longitudinal control channels. This result is used to design small-signal linear multivariable regulators for the two control channels. The linear compensators also entail integral action. Thus, the controller consists of a strongly nonlinear feedforward module and a linear multivariable small-signal compensator. The novel multivariable set point controller encompasses full three-axes autopilot functions. Moreover, this controller is used as a dynamic phugoid damping controller, provided that the bandwidth of the command signal is substantially less than the bandwidth of the closed-loop flight control system. Hence, the bandwidth of the closed-loop phugoid damping control system is maximized, while at the same time due attention is given to the control signals' excursions. Section IV presents the results of simulations for the phugoid damping controller's performance evaluation. The wide operational envelope of the controller is demonstrated. Concluding remarks are made in Sec. V.

Table 1 Aircraft parameter values

Parameter	Value
Wing lift curve slope a_W	5.3 /rad
Tail lift curve slope a_T	5.3 /rad
Wing aspect ratio AR	3
Wing span, b	9.14 m
Zero-lift drag coefficient C_{D0}	0.015
Acceleration of gravity g	9.81 m/s^2
Parabolic drag polar constant K	0.1118
Mass m	11,336.4 kg
Dynamic pressure $\bar{q}$	12,500 kg/(m $\cdot$ s^2)
Wing surface area S_W	27.87 m^2
Tail surface area S_T	5.086 m^2
Initial velocity V_0	200 m/s
Efficiency factor η	0.95
Atmospheric density (at 20,000 ft) ρ	$\frac{5}{8}$ kg/m^3

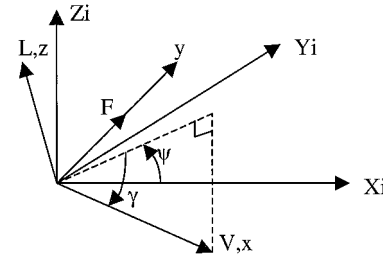

Fig. 1 Wind axes x, y, and z.

II. Equations of Motion and Trim Control Laws

The aircraft's point-mass equations of motion are derived using a translating and rotating frame of reference collocated with the instantaneous position of the aircraft. The rotating frame of reference, shown in Fig. 1, is a triad of wind axes defined as follows: The x axis is aligned with the aircraft velocity vector, the z axis is aligned with the lift vector, and the y axis (out of the wing) completes the right-handed coordinate system. The wind axes frame's attitude is specified by the ψ, γ, and ϕ Euler angles, corresponding to the aircraft heading, flight-path angle (in the pitch plane), and roll angle. For the sake of clarity, the final rotation about the x axis through the angle ϕ is not explicitly shown in Fig. 1. Also, velocity vector rolls are envisaged because the roll maneuver is performed about the velocity vector axis.

The three angles ψ, γ, and ϕ are not unlike the Euler angles; they position the wind axes frame x, y, z relative to the inertial frame X_I, Y_I, Z_I. Note, however, that, whereas the heading angle ψ and the flight-path angle γ are state variables, the bank angle ϕ is a control variable. Also note the polarity of the flight-path angle γ, as indicated in Fig. 1.

A. Aerodynamic Angles Definition

In this paper, wind axes, rather than body axes, are used. However, a discussion of body axes is required to define the aerodynamic angles properly. Thus, the body axes triad, X_b, Y_b, and Z_b, is related to the wind axes, x, y, and z, as follows: Initially, the body axes are aligned with the wind axes. First, a rotation of β degrees about the z wind axis is performed. This is followed by a rotation of α degrees about the Y_b body axis. The broken line X_b' in Fig. 2 is the projection of the X_b axis onto the (x, y) plane. We note that

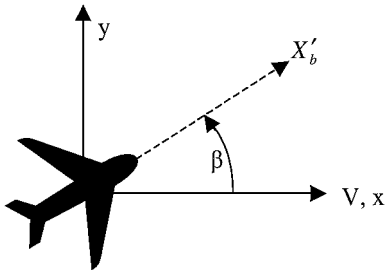

Fig. 2 Sideslip angle definition.

this definition of aerodynamic angles is not the standard definition used when body axes and rigid-body dynamics are used to describe the aircraft's motion. At the same time, the aerodynamic angles just defined correspond to the aerodynamic angles used in wind-tunnel work. Because a point-mass model is used, moments are not included in the analysis.

B. Equations of Motion

The aircraft dynamic model used in this paper exclusively employs the aircraft's slow states and is, therefore, the right model for model-based outer-loop controller design, namely, altitude-hold, Mach-hold, and heading-hold autopilot design, and for phugoid damping controller design.

The point-mass equations of motion (see, for example, Fig. 1 and Ref. 8) are

$$\dot{V} = \frac{T - D}{m} + g\sin\gamma, \qquad V(0) = V_0$$

$$\dot{\gamma} = -\frac{L\cos\phi + F\sin\phi}{mV} + \frac{g}{V}\cos\gamma, \qquad \gamma(0) = \gamma_0$$

$$\dot{\psi} = \frac{-L\sin\phi + F\cos\phi}{mV\cos\gamma}, \qquad \Psi(0) = 0, \qquad 0 \le t \le t_{\max}$$

where the forces are

$$L = \bar{q}\left(V^2/V_0^2\right)S_W a_W \alpha, \qquad T = mg\mu$$

$$D = \bar{q}\left(V^2/V_0^2\right)S_W\left(C_{D0} + Ka_W^2\alpha^2\right), \qquad F = \bar{q}\left(V^2/V_0^2\right)S_t a_t \beta$$

and where the nominal dynamic pressure is

$$\bar{q} = \tfrac{1}{2}\rho \cdot V_0^2$$

and V_0 is the initial velocity. The pertinent F-16 class aircraft parameters are given in Table 1.

Remark: For constant altitude and wings level flight, the trim lift coefficient $\bar{C}_L = \tilde{C}_L$. Hence, the trim lift-over-drag ratio is given by

$$\bar{C}_L/\bar{C}_D = 1/(C_{D0}\bar{q} + K)$$

Nondimensional variables and parameters are introduced as follows:

$$t := (g/V_0)t, \qquad V := V/V_0, \qquad \bar{\omega} := (V_0/g)\bar{\omega}$$

$$\bar{q} := \bar{q}S_W/m \cdot g, \qquad \tilde{C}_L \equiv 1/\bar{q}, \qquad K := K\tilde{C}_L$$

$$\tilde{\alpha} := \tilde{C}_L/a_W, \qquad \alpha := \alpha/\tilde{\alpha}, \qquad \beta := (1/\tilde{\alpha})(S_t/S_W)(a_t/a_W)\cdot\beta$$

Similarly, the (barred) trim controls are scaled according to

$$\bar{\alpha} := \bar{\alpha}/\tilde{\alpha}, \qquad \bar{\beta} := (1/\tilde{\alpha})(S_t/S_W)(a_t/a_W)\cdot\bar{\beta}$$

The nondimensional parameters and variables are given in Table 2.

By use of the preceding parameterization in the point-mass equations of motion, the elegant nondimensional aircraft equations of motion are derived:

$$\dot{V} = \sin\gamma - \bar{q}C_{D0}V^2 + \mu - KV^2\alpha^2, \qquad V(0) = 1 \qquad (1)$$

$$\dot{\gamma} = \cos\gamma/V - V(\alpha\cos\phi + \beta\sin\phi), \qquad \gamma(0) = \gamma_0 \qquad (2)$$

$$\dot{\psi} = (V/\cos\gamma)(-\alpha\sin\phi + \beta\cos\phi), \qquad \psi(0) = 0$$

$$0 \le t \le t_{\max} \qquad (3)$$

Table 2 Nondimensional parameters and variables

Parameter	Actual	Nondimensional
$\tilde{C}_L$	——	0.319
$\bar{C}_L/\bar{C}_D$	——	12.1
K	0.112	0.0357
$\bar{q}$	12,500 kg/(m · s^2)	3.13
t	t, s	0.0491t
V	V, m/s	0.05V
α	α	16.6α
$\tilde{\alpha}$	——	0.0602
β	β	3.03β
$\bar{\omega}$	$\bar{\omega}$, s^{-1}	20.4$\bar{\omega}$
ω_n	0.0694, s^{-1}	$\sqrt{2}$

The two parameters in the equations of motion (1) are $(\bar{q}C_{D0})$ and K, where, for the flight condition considered in the paper, the numerical values are $\bar{q}C_{D0} = 0.04695$ and $K = 0.0357$.

C. Aircraft Trim Equations

The equations of motion reported in the preceding section define velocity V, flight-path angle γ, and heading ψ in terms of thrust setting μ, angle of attack α, bank angle ϕ, and sideslip angle β. Thus, V, γ, and ψ are the states, and the control variables are μ, α, ϕ, and β. To use these control variables to bring about a desired state, it is necessary to know to what values the control variables should be set.

The controller's design will be based on the idea that attaining a commanded steady state, or trim state, is the desired condition. Determining the trim control signals requires setting the derivatives of the state variables, $\dot{V}$ and $\dot{\gamma}$, to zero, and $\dot{\psi} = -\bar{\omega}$ or $\psi(t) = -\bar{\omega}\cdot t$. The trimmed aircraft flies at constant speed, holds a constant flight-path angle, and maintains a constant heading rate, that is, it is maintaining a steady turn. This allows the aircraft to come to a trim state in which it is holding speed and flight-path angle and maintaining a steady turn.

The new trim values $\psi(t) = -\bar{\omega}\cdot t$, $\bar{\gamma}$, and $\bar{V}$ are commanded. The corresponding trim control settings are $\bar{\mu}$, $\bar{\alpha}$, $\bar{\phi}$, and $\bar{\beta}$. Here, $\bar{\omega} > 0$, that is, without loss of generality, we consider a turn to starboard, so that the ensuing trim bank angle $\bar{\phi} > 0$. Again, all variables are nondimensionalized.

Equations (1) and (2) are considered first. Now, setting the left-hand side of the differential equations (1) and (2) equal to 0 yields

$$\bar{\alpha}\sin\bar{\phi} - \bar{\beta}\cos\bar{\phi} = (\bar{\omega}/\bar{V})\cos\bar{\gamma}$$

$$\bar{\alpha}\cos\bar{\phi} + \bar{\beta}\sin\bar{\phi} = (1/\bar{V}^2)\cos\bar{\gamma} \qquad (4)$$

This is a system of two nonlinear equations in the unknowns $\bar{\alpha}$ and $\bar{\phi}$; in Eqs. (4), $\bar{V}$, $\bar{\beta}$, and $\bar{\gamma}$ are parameters. The explicit trim solution is

$$\bar{\beta} = K_{\bar{\beta},\bar{\omega}}\cdot(-\bar{\omega}), \qquad \bar{\alpha} = \sqrt{\frac{\cos^2\bar{\gamma}}{\bar{V}^4}(1 + \bar{\omega}^2\bar{V}^2) - K_{\bar{\beta},\bar{\omega}}^2\bar{\omega}^2}$$

$$\bar{\mu} = \bar{q}\bar{V}^2C_{D0} - \sin\bar{\gamma} + \frac{K}{\bar{V}^2}(1 + \bar{\omega}^2\bar{V}^2)\cos^2\bar{\gamma} - K\bar{V}^2K_{\bar{\beta},\bar{\omega}}^2\bar{\omega}^2$$

$$\sin\bar{\phi} = \frac{\bar{V}^2}{1 + \bar{\omega}^2\bar{V}^2}\frac{1}{\cos\bar{\gamma}} \times\left[\bar{\omega}\bar{V}\sqrt{\frac{1 + \bar{\omega}^2\bar{V}^2}{\bar{V}^4}\cos^2\bar{\gamma} - K_{\bar{\beta},\bar{\omega}}^2\bar{\omega}^2} - K_{\bar{\beta},\bar{\omega}}\bar{\omega}\right]$$

$$\cos\bar{\phi} = \frac{\bar{V}^2}{1 + \bar{\omega}^2\bar{V}^2}\frac{1}{\cos\bar{\gamma}} \times\left[\sqrt{\frac{1 + \bar{\omega}^2\bar{V}^2}{\bar{V}^4}\cos^2\bar{\gamma} - K_{\bar{\beta},\bar{\omega}}^2\bar{\omega}^2} + K_{\bar{\beta},\bar{\omega}}\bar{\omega}^2\bar{V}\right] \qquad (5)$$

It is remarkable that the aerodynamic controls $\bar{\alpha}$ and $\bar{\phi}$ are not dependent on the problem parameters $(\bar{q}C_{D_0})$ and K. The throttle setting $\bar{\mu}$ is, however, dependent on the problem parameters $(\bar{q}C_{D_0})$ and K.

A reasonable choice for the gain $K_{\bar{\beta},\bar{\omega}}$ is

$$K_{\bar{\beta},\bar{\omega}} = 0.05$$

Indeed, the following holds:

$$3.03\bar{\beta} = K_{\bar{\beta},\bar{\omega}} \cdot 20.4 \cdot \bar{\omega}$$

where $\bar{\beta}$ and $\bar{\omega}$ are the physical (original) variables.

For $\bar{\omega} = 15$ deg/s, use $\bar{\beta} = 5$ deg $\rightarrow 3.03 \cdot 5 = K_{\bar{\beta},\bar{\omega}} \cdot 20.4 \cdot 15 \rightarrow K_{\bar{\beta},\bar{\omega}} = 3.03/20.4 \cdot 3 \approx 0.05$.

Remarks: For coordinated bank-to-turn (BTT) turns, there is no sideslip angle; choose

$$K_{\bar{\beta},\bar{\omega}} = 0$$

Conversely, for skid-to-turn (STT) control there is no bank; set

$$\bar{\phi} = 0$$

which leads to

$$\bar{\alpha} = (1/\bar{V}^2)\cos\bar{\gamma}, \qquad \bar{\beta} = -(\bar{\omega}/\bar{V})\cos\bar{\gamma}$$

$$\bar{\mu} = C_{D0}\bar{q}\bar{V}^2 - \sin\bar{\gamma} + (K/\bar{V}^2)\cos^2\bar{\gamma} \tag{6}$$

If $\bar{\phi}$ is independently controlled, for example, to point the aircraft to facilitate the solution of the fire control problem, the trim equations are

$$\begin{bmatrix} \cos\bar{\phi} & \sin\bar{\phi} \\ -\sin\bar{\phi} & \cos\bar{\phi} \end{bmatrix} \begin{pmatrix} \bar{\alpha} \\ \bar{\beta} \end{pmatrix} = \frac{1}{\bar{V}^2}\cos\bar{\gamma} \begin{pmatrix} 1 \\ -\bar{\omega}\bar{V} \end{pmatrix}$$

whereupon the solution is obtained:

$$\bar{\alpha} = (1/\bar{V}^2)(\cos\bar{\phi} + \bar{\omega}\bar{V}\sin\bar{\phi})\cos\bar{\gamma}$$

$$\bar{\beta} = (1/\bar{V}^2)(\sin\bar{\phi} - \bar{\omega}\bar{V}\cos\bar{\phi})\cos\bar{\gamma}$$

$$\bar{\mu} = C_{D0}\bar{q}\bar{V}^2 - \sin\bar{\gamma} + (K/\bar{V}^2)(\bar{\omega}\bar{V}\sin\bar{\phi} + \cos\bar{\phi})^2\cos^2\bar{\gamma} \tag{7}$$

III. Small Signal Control Law and Complete Control Law

The control concept is now introduced. Because the plant is nonlinear and must be operated about a nonzero set point, a nonlinear feedforward design is implemented in parallel with a small-signal linear feedback controller. Hence, the aircraft model must be linearized so that a small-signal linear controller can be designed.

A. Linearization

Linearization of the aircraft nonlinear dynamics (1–3) about the trim condition ($\bar{V} = 1, \bar{\gamma} = 0, \bar{\psi} = 0$) produced the dynamics matrix

$$A = \left[\begin{array}{cc:c} -2/(\bar{C}_L/\bar{C}_D) & 1 & 0 \\ -2 & 0 & 0 \\ \hdashline 0 & 0 & 0 \end{array}\right]$$

and the control matrix

$$B = \left[\begin{array}{cc:cc} 1 & -2K & 0 & 0 \\ 0 & -1 & 0 & 0 \\ \hdashline 0 & 0 & -1 & 1 \end{array}\right]$$

B. Theory

The feedforward portion, the trim solver, is based on the nonlinear aircraft trim equations derived in Sec. II. Consider now the nonlinear dynamics:

$$\dot{x} = f(x,u), \qquad x(0) = x_0, \qquad x, x_0 \in \Re^n$$

$$u \in \Re^m, \qquad y = x, \qquad 0 \le t$$

and the reference signal:

$$r = \bar{x}$$

where $\bar{x}$ is a rest point (or equilibrium point, or trim point) of the dynamic system. Consider the set of trim points of interest $X \subset \Re^n$.

Hypothesis:

$$\forall\, \bar{x} \in X \;\exists\, \bar{u} \in \Re^m \qquad \text{so that} \qquad f(\bar{x},\bar{u}) = 0$$

Moreover, under mild assumptions on f, $\exists$ smooth function g: $\Re^n \rightarrow \Re^m$ so that

$$\bar{u} = g(\bar{x})$$

by the implicit function theorem. In other words,

$$f[\bar{x}, g(\bar{x})] = 0, \qquad \forall\, \bar{x} \in X$$

Given the reference signal $r = \bar{x}$ ($\equiv$ const), consider the control law

$$u = g(r) - v$$

where v is the output of the linear controller. The dynamics then are

$$\dot{x} = f[x, g(\bar{x}) - v], \qquad x(0) = x_0, \qquad 0 \le t, \qquad y = x$$

We linearize the function f about the trim point $[\bar{x}, g(\bar{x})]$. Thus,

$$f[x, g(\bar{x}) - v] = f[\bar{x}, g(\bar{x})] + A(x - \bar{x}) - Bv$$

$$+ \text{higher-order terms} = 0 + A(x - \bar{x}) - Bv + d$$

where

$$A \equiv \left.\frac{\partial f}{\partial x}\right|_{[\bar{x},g(\bar{x})]}, \qquad B \equiv \left.\frac{\partial f}{\partial u}\right|_{[\bar{x},g(\bar{x})]}, \qquad d \equiv \text{higher-order terms}$$

Hence, the perturbation dynamics are

$$\dot{e} = Ae + Bv + d$$

where

$$e \equiv r - y = \bar{x} - x$$

Tracking of a constant command signal r is guaranteed, provided that the control signal v is generated by a stabilizing state feedback control law.

We will use a proportional-integral control law. We need integral action because we need to reject the linearization-induced disturbance d (Ref. 9). Moreover, although we do not need integral action for tracking the constant set point command when the linearized dynamics with $d = 0$ are used, integral action might also help when tracking a dynamic reference signal. Hence, we augment the perturbation dynamics as follows:

$$\dot{e} = Ae + Bv + d, \qquad \dot{z} = e$$

where z is the charge on the integrator.

Use the linear control law

$$v = K_P e + K_I z$$

In matrix form, the closed-loop dynamics are

$$\frac{\mathrm{d}}{\mathrm{d}t}\begin{bmatrix} e \\ z \end{bmatrix} = \begin{bmatrix} A & 0 \\ I & 0 \end{bmatrix}\begin{bmatrix} e \\ z \end{bmatrix} + \begin{bmatrix} B \\ 0 \end{bmatrix} v + \begin{bmatrix} I \\ 0 \end{bmatrix} d$$

and the linear controller output is

$$v = [K_P \quad K_I]\begin{pmatrix} e \\ z \end{pmatrix}$$

Hence, the small-signal dynamics are governed by

$$\frac{\mathrm{d}}{\mathrm{d}t}\begin{pmatrix} e \\ z \end{pmatrix} = \begin{bmatrix} A + BK_P & BK_I \\ I & 0 \end{bmatrix}\begin{pmatrix} e \\ z \end{pmatrix} + \begin{bmatrix} I \\ 0 \end{bmatrix} d, \qquad \begin{aligned} e(0) &= e_0 \\ z(0) &= 0 \end{aligned}$$

Remark: We want $e \to 0$ ($\equiv$ tracking). This implies $BK_I z + d = 0$. Because d is arbitrary, need (BK_I) invertible $\to$ need B and K_I invertible.

Now,

$$\det\left(\begin{bmatrix} A + BK_P & BK_I \\ I & 0 \end{bmatrix}\right) = \det(BK_I)$$

Hence, we conclude that the dynamics matrix

$$\begin{bmatrix} A + BK_P & BK_I \\ I & 0 \end{bmatrix}$$

does not have zero eigenvalues. Moreover, we require

$$\begin{bmatrix} A + BK_P & BK_I \\ I & 0 \end{bmatrix}$$

to be a stability matrix, that is, a matrix whose eigenvalues all have strictly negative real parts. This is not a problem because the poles of the open-loop system

$$\begin{bmatrix} A & 0 \\ I & 0 \end{bmatrix}$$

are assignable. Indeed, the pair

$$\left(\begin{bmatrix} A & 0 \\ I & 0 \end{bmatrix}, \begin{bmatrix} B \\ 0 \end{bmatrix}\right)$$

is controllable. Thus,

$$\operatorname{rank}\left(\left[\begin{array}{c|c} B & AB \\ 0 & B \end{array}\right]\right) = 2n$$

because B is an $n \times m$ full-rank ($=n$) matrix.

Furthermore,

$$\begin{bmatrix} A + BK_P & BK_I \\ I & 0 \end{bmatrix}$$

a stability matrix $\to A + BK_P$ a stability matrix. Again, the poles of the pair (A, B) are assignable because (A, B) is a controllable pair (because the $n \times n$ matrix B is nonsingular.)

Hence, we first design the proportional controller. This governs the tracking error dynamics. The second step entails the setting of the integral gains. Note that integral action is not strictly needed when 1) there are no disturbances, namely, when the linearized dynamics are used and 2) the reference signal $r = \bar{x} \equiv$ const.

C. Phugoid Damping Controller

The complete phugoid damping control system's block diagram is shown in Fig. 3. Here, $y = x$, $e = r - y$, $\dot{z} = e$, $z(0) = 0$, and $u = g(r) - K_P e - K_I z$, where, we recall,

$$r = \begin{pmatrix} \bar{v} \\ \bar{\gamma} \\ \bar{\psi} \end{pmatrix}, \qquad x = \begin{pmatrix} v \\ \gamma \\ \psi \end{pmatrix}, \qquad u = \begin{pmatrix} \mu \\ \alpha \\ \phi \\ \beta \end{pmatrix}$$

zooming in on the ψ-channel (see Fig. 4).

The function $g(\cdot)$ implements the nonlinear trim signal calculation developed in Sec. III. The nonlinear trim function $g(\cdot)$ is explicitly specified as follows:

$$\begin{pmatrix} \bar{\mu} \\ \bar{\alpha} \\ \bar{\phi} \end{pmatrix} = g(\bar{v}, \bar{\gamma}, \bar{\omega}; \bar{\beta})$$

where [see Eqs. (5)]

$$\bar{\mu} = \bar{q} C_{D0} \bar{V}^2 - \sin\bar{\gamma} + \frac{K}{\bar{V}^2}\cos^2\bar{\gamma}(1 + \bar{\omega}^2\bar{V}^2) - K\bar{\beta}^2\bar{V}^2$$

$$\bar{\alpha} = \sqrt{\frac{\cos^2\bar{\gamma}}{\bar{V}^4}(1 + \bar{\omega}^2\bar{V}^2) - \bar{\beta}^2}$$

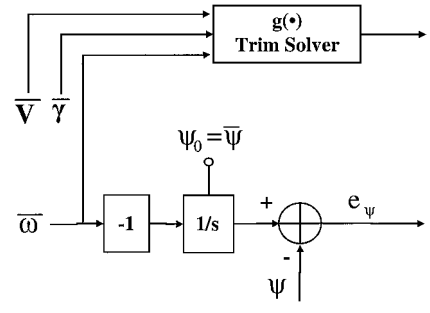

Fig. 4 Block diagram of ψ-channel.

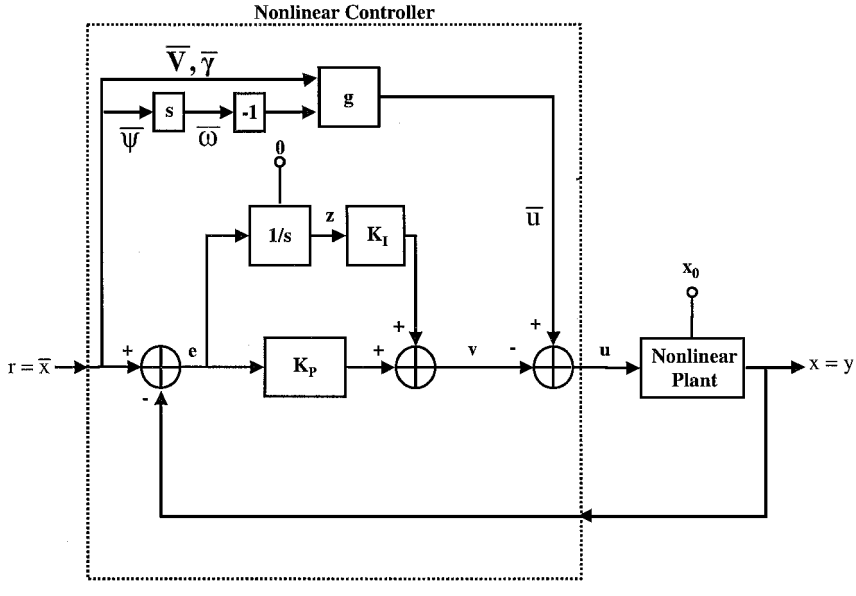

Fig. 3 Phugoid damping control system.

Table 3 Desired parameters of lateral FCS channel

Parameter	Dimensional	Nondimensional
τ	10 s	0.49
ξ_P	$\frac{\sqrt{2}}{2}$	$\frac{\sqrt{2}}{2}$
ω_{n_P}	$\sqrt{2}(g/V_0)$	$\sqrt{2}$

$$\sin\bar{\phi} = \frac{\bar{V}^2}{\cos\bar{\gamma}}\frac{1}{1+\bar{\omega}^2\bar{V}^2}\left[\bar{\omega}\bar{V}\sqrt{\frac{\cos^2\bar{\gamma}}{\bar{V}^4}(1+\bar{\omega}^2\bar{V}^2)-\bar{\beta}^2}+\bar{\beta}\right]$$

$$\cos\bar{\phi} = \frac{\bar{V}^2}{\cos\bar{\gamma}}\frac{1}{1+\bar{\omega}^2\bar{V}^2}\left[\sqrt{\frac{\cos^2\bar{\gamma}}{\bar{V}^4}(1+\bar{\omega}^2\bar{V}^2)-\bar{\beta}^2}-\bar{\omega}\bar{V}\bar{\beta}\right]$$

D. Proportional Control

The controller's design is based on the linearized special case of trimmed, wings level, constant altitude flight, with trim speed equal to initial speed. Proportional controllers are designed separately for both lateral and longitudinal channel control, and integral action is added to the lateral channel.

1. *Lateral/Directional Channel*

The desired flight control system (FCS) lateral channel's aircraft control parameters are specified in Table 3.

Note that the lateral/directional control channels' nondimensional time constant is

$$\tau := \tau\cdot(g/V_0)$$

In the lateral/directional channel, the reference signal is $\bar{\psi}$, and, thus, the error signal is

$$e_\psi \equiv \bar{\psi}-\psi \text{ [rad]}$$

The linearized lateral directional equation of motion is

$$\dot{e}_\psi = -\phi+\beta$$

The controls are

$$\phi = K_{\phi,\psi}\cdot e_\psi, \qquad \beta = K_{\beta,\psi}\cdot e_\psi$$

$\rightarrow$

$$\dot{e}_\psi = -K_{\phi,\psi}e_\psi + K_{\beta,\psi}e_\psi = -(K_{\phi,\psi}-K_{\beta,\psi})e_\psi$$

$\rightarrow$

$$e_\psi(t) = \exp[-(K_{\phi,\psi}-K_{\beta,\psi})t]e_\psi(0)$$

We want $e_\psi(t) = e^{-t/\tau}e_\psi(0)$. Hence, set

$$K_{\phi,\psi}-K_{\beta,\psi} = 1/\tau$$

Note that τ is the specified nondimensional directional time constant.

Choosing a dimensional $\tau = 10$ s $\rightarrow$ nondimensional $\tau = 0.5$:

$$\rightarrow \qquad K_{\phi,\psi}-K_{\beta,\psi} = 2 \tag{8}$$

If a BTT control strategy is employed, then $K_{\beta,\psi}=0$

$$\rightarrow \qquad K_{\phi,\psi} = 2 \tag{9}$$

If, instead, an STT control strategy is used, then $K_{\phi,\psi}=0$

$$\rightarrow \qquad K_{\beta,\psi} = -2 \tag{10}$$

2. *Longitudinal Channel*

The reference signals are $\bar{V}$ and $\bar{\gamma}$, and, thus, the error signals are

$$e_V \equiv \bar{V}-V, \qquad e_\gamma \equiv \bar{\gamma}-\gamma \text{ [rad]}$$

which are fed back to the linear controller. Thus, the linear controller operates on feedback signals e_v and e_γ. The control variables for the aircraft longitudinal channel are α and μ. We need to specify the four controller gains $K_{\alpha V}$, $K_{\alpha\gamma}$, $K_{\mu V}$, and $K_{\mu\gamma}$. We will use ω_{n_P} (longitudinal channel's natural frequency) and ξ_p (longitudinal channel's damping ratio) as the longitudinal channel's design specifications.

The design equations are derived as follows: The closed-loop system's dynamics matrix is

$$A_{\text{cl}_P} = \begin{bmatrix} -2(\bar{C}_D\bar{C}_L)+K_{\mu V}-2K\cdot K_{\alpha V} & 1+K_{\mu\gamma}-2K\cdot K_{\alpha\gamma} \\ -2-K_{\alpha V} & -K_{\alpha\gamma}\end{bmatrix}$$

Hence, the design equations are

$$\text{tr}\left(A_{\text{cl}_P}\right) = -2\xi_P\omega_{n_P}, \qquad \det\left(A_{\text{cl}_P}\right) = \omega_{n_P}^2$$

Thus, the design equations yield two equations in four unknowns (the gains $K_{\alpha V}$, $K_{\alpha\gamma}$, $K_{\mu V}$, and $K_{\mu\gamma}$):

$$K_{\alpha\gamma}+2K\cdot K_{\alpha V}-K_{\mu V} = 2\left(\xi_P\omega_{n_P}-\bar{C}_D/\bar{C}_L\right)$$

$$K_{\alpha\gamma}[2K\cdot K_{\alpha V}-K_{\mu V}+2(\bar{C}_D/\bar{C}_L)] + (2+K_{\alpha V})(1+K_{\mu\gamma}-2K\cdot K_{\alpha\gamma}) = \omega_{n_P}^2$$

The first equation yields

$$2K\cdot K_{\alpha V}-K_{\mu V}+2(\bar{C}_D/\bar{C}_L) = 2\xi_P\omega_{n_P}-K_{\alpha\gamma}$$

Inserting this expression in the second equation yields

$$K_{\alpha\gamma}\left(2\xi_P\omega_{n_P}-K_{\alpha\gamma}\right)+(2+K_{\alpha V})(1+K_{\mu\gamma}-2K\cdot K_{\alpha\gamma}) = \omega_{n_P}^2$$

Hence, we have obtained the two design equations:

$$K_{\alpha\gamma}+2KK_{\alpha V}-K_{\mu V} = 2\left(\xi_P\omega_{n_P}-\bar{C}_D/\bar{C}_L\right) \tag{11}$$

$$K_{\alpha\gamma}\left(2\xi_P\omega_{n_P}-K_{\alpha\gamma}\right)+(2+K_{\alpha V})(1+K_{\mu\gamma}-2KK_{\alpha\gamma}) = \omega_{n_P}^2 \tag{12}$$

In summary, we have two equations in the four unknowns $K_{\alpha V}$, $K_{\alpha\gamma}$, $K_{\mu V}$, and $K_{\mu\gamma}$. In the design equations, only the problem parameter K is featured, as are, of course, the design specifications ξ_P and ω_{n_P}.

Finally, the complete control law is

$$\mu = \bar{q}\bar{V}^2C_{D0}-\sin\bar{\gamma}+\frac{K}{\bar{V}^2}(1+\bar{\omega}^2\bar{V}^2)\cos^2\bar{\gamma} - K\bar{V}^2K_{\bar{\beta},\bar{\omega}}^2\bar{\omega}^2-K_{\mu V}\cdot e_V-K_{\mu\gamma}\cdot e_\gamma$$

$$\alpha = \sqrt{\frac{\cos^2\bar{\gamma}}{\bar{V}^4}(1+\bar{\omega}^2\bar{V}^2)-K_{\bar{\beta},\bar{\omega}}^2\bar{\omega}^2}-K_{\alpha V}\cdot e_V-K_{\alpha\gamma}\cdot e_\gamma$$

$$\phi = A\sin\left\{\frac{\bar{V}^2}{1+\bar{\omega}^2\bar{V}^2}\frac{1}{\cos\bar{\gamma}}\cdot\left[\bar{\omega}\bar{V}\sqrt{\frac{1+\bar{\omega}^2\bar{V}^2}{\bar{V}^4}\cos^2\bar{\gamma}-K_{\bar{\beta},\bar{\omega}}^2\bar{\omega}^2} - K_{\bar{\beta},\bar{\omega}}\bar{\omega}\right]\right\}-K_{\phi,\psi}\cdot e_\psi$$

$$\beta = K_{\bar{\beta},\bar{\omega}}\cdot(-\bar{\omega})-K_{\beta,\psi}e_\psi$$

Choose $K_{\alpha V}=0$ and $K_{\mu\gamma}=0$. Within the controller, velocity error has no effect on angle of attack (AOA), and flight-path angle error has no effect on thrust setting. This implies that AOA is exclusively controlled by the error in flight-path angle e_γ, whereas thrust setting is controlled solely using velocity error e_V. Thus, the design equations (11) and (12) are now

$$K_{\alpha\gamma}-K_{\mu V} = 2\left(\xi_P\omega_{n_P}-\bar{C}_D/\bar{C}_L\right)$$

$$2\xi_P\omega_{n_P}K_{\alpha\gamma}-K_{\alpha\gamma}^2+2-4KK_{\alpha\gamma} = \omega_{n_P}^2$$

Hence, we have two equations in the two unknowns $K_{\alpha\gamma}$ and $K_{\mu V}$. The second design equation is a quadratic equation in $K_{\alpha\gamma}$:

$$K_{\alpha\gamma}^2 + 2\big(2K - \xi_P\omega_{n_P}\big)K_{\alpha\gamma} + \omega_{n_P}^2 - 2 = 0$$

$$\rightarrow$$

$$K_{\alpha\gamma} = \xi_P\omega_{n_P} - 2K \pm \sqrt{\big(\xi_P^2 - 1\big)\omega_{n_P}^2 + 2 + 4K^2 - 4K\xi_P\omega_{n_P}}$$

$$K_{\mu V} = 2(\bar{C}_D/\bar{C}_L) - 2K - \xi_P\omega_{n_P} \pm \sqrt{\big(\xi_P^2 - 1\big)\omega_{n_P}^2 + 2 + 4K^2 - 4K\xi_P\omega_{n_P}}$$

If we were to specify

$$\xi_P = \sqrt{2}/2$$

then the two solutions are

$$K_{\alpha\gamma} = \big(\sqrt{2}/2\big)\omega_{n_P} - 2K + \sqrt{\big[\big(\sqrt{2}/2\big)\omega_{n_P} - 2K\big]^2 + 2 - \omega_{n_P}^2}$$

$$K_{\mu V} = 2(\bar{C}_D/\bar{C}_L) - \big(\sqrt{2}/2\big)\omega_{n_P} - 2K + \sqrt{\big[\big(\sqrt{2}/2\big)\omega_{n_P} - 2K\big]^2 + 2 - \omega_{n_P}^2} \tag{13}$$

$$K_{\alpha\gamma} = \big(\sqrt{2}/2\big)\omega_{n_P} - 2K - \sqrt{\big[\big(\sqrt{2}/2\big)\omega_{n_P} - 2K\big]^2 + 2 - \omega_{n_P}^2}$$

$$K_{\mu V} = 2(\bar{C}_D/\bar{C}_L) - \big(\sqrt{2}/2\big)\omega_{n_P} - 2K - \sqrt{\big[\big(\sqrt{2}/2\big)\omega_{n_P} - 2K\big]^2 + 2 - \omega_{n_P}^2} \tag{14}$$

We want to increase the bandwidth of the closed-loop FCS to enhance tracking performance. Hence, we will specify $\omega_{n_P} \geq \omega_n = \sqrt{2}$.

This choice of ω_n and ξ effectively changes the damping of the closed-loop system while retaining the natural frequency of the open-loop system. Because settling time is related to natural frequency, system response can be improved by increasing the natural frequency. Therefore, we increase the desired natural frequency to, for example, $\omega_{n_P} = \sqrt{3}$. Note that ω_{n_P} could be increased further, at the expense of increasing the gains of the controller. Note also that, in each case, three of the four gains are set to approximately zero. These are particularly low-gain controllers. This is not surprising, given the limited design requirements given.

Remark: A physically realizable controller matrix is required to use real gains. A negative discriminant would produce complex gains. We need a nonnegative discriminant, namely,

$$\big[\big(\sqrt{2}/2\big)\omega_{n_P} - 2K\big]^2 \geq \omega_{n_P}^2 - 2$$

$$\rightarrow$$

$$0 < \omega_{n_P} < 2\big(\sqrt{1 + 4K^2} - \sqrt{2}K\big)$$

Hence, choose, for example,

$$\omega_{n_P} = \sqrt{3}$$

Then, using the solution provided by Eqs. (13),

$$K_{\alpha\gamma} = \big(1/\sqrt{2}\big)\Big(\sqrt{1 - 4\sqrt{6}K + 8K^2} + \sqrt{3} - 2\sqrt{2}K\Big)$$

$$K_{\mu V} = 2(\bar{C}_D/\bar{C}_L) + \big(1/\sqrt{2}\big)\Big(\sqrt{1 - 4\sqrt{6}K + 8K^2} - \sqrt{3} - 2\sqrt{2}K\Big)$$

Thus, $K_{\alpha\gamma} > 0$ and $K_{\mu V} < 0$, as required.

In general, one can choose $K_{\mu V} \neq 0$ and the pitch channel small-signal linear controller can be a four gains controller.

E. Integral Action Control

Let

$$e \equiv \begin{pmatrix} v_e \\ \gamma_e \\ \psi_e \end{pmatrix} \in \Re^3, \qquad z \equiv \begin{pmatrix} z_V \\ z_\gamma \\ z_\psi \end{pmatrix} \in \Re^3, \qquad d \equiv \begin{pmatrix} d_v \\ d_\gamma \\ d_\psi \end{pmatrix} \in \Re^3$$

where e is the error signal, z is the integrator charge, and d is the disturbance signal.

We analyze and simulate the linear system

$$\dot{e} = Ae + Bv + d, \qquad e(0) = e_0, \qquad \dot{z} = e, \qquad z(0) = 0$$

where

$$A = \left[\begin{array}{cc:c} -2/(\bar{C}_L/\bar{C}_D) & 1 & 0 \\ -2 & 0 & 0 \\ \hdashline 0 & 0 & 0 \end{array}\right], \qquad B = \left[\begin{array}{cc:cc} 1 & -2K & 0 & 0 \\ 0 & -1 & 0 & 0 \\ \hdashline 0 & 0 & -1 & 1 \end{array}\right]$$

First consider the BTT scenario, where $\beta \equiv 0$ and, thus,

$$v \equiv \begin{pmatrix} \mu \\ \alpha \\ \beta \end{pmatrix}$$

and B is a 3×3 matrix. The control signal is formed according to

$$v = K_P e + K_I v$$

where the gains are

$$K_P = \left[\begin{array}{cc:c} K_{\mu,V} & K_{\mu,\gamma} & 0 \\ K_{\alpha,V} & K_{\alpha,\gamma} & 0 \\ \hdashline 0 & 0 & K_{\phi,\psi} \end{array}\right]$$

$$K_I = \left[\begin{array}{cc:c} K_{\mu,z_V} & K_{\mu,z_\gamma} & 0 \\ K_{\alpha,z_V} & K_{\alpha,z_\gamma} & 0 \\ \hdashline 0 & 0 & K_{\phi,z_\psi} \end{array}\right]$$

Hence, the closed-loop control system is described by

$$\frac{\mathrm{d}}{\mathrm{d}t}\begin{pmatrix} e \\ z \end{pmatrix} = \begin{pmatrix} A + BK_P & BK_I \\ I_3 & 0_3 \end{pmatrix}\begin{pmatrix} e \\ z \end{pmatrix} + \begin{pmatrix} I_3 \\ 0_3 \end{pmatrix} d, \qquad \begin{matrix} e(0) = e_0 \\ z(0) = 0 \end{matrix}$$

The system is composed of two independent channels, lateral and longitudinal. The two channels can be decoupled in the same manner as was done in the proportional controller. The lateral/directional channel dynamics are

$$\dot{\psi}_e = -K_{\phi,\psi}\psi_e - K_{\phi,z_\psi}z_\psi + d_\psi, \qquad \psi_{e_0}(0) = r_\psi$$
$$\dot{z}_\psi = \psi_e, \qquad z_\psi(0) = 0$$

that is,

$$\frac{\mathrm{d}}{\mathrm{d}t}\begin{pmatrix} \psi_e \\ z_\psi \end{pmatrix} = \begin{pmatrix} -K_{\phi,\psi} & -K_{\phi,z_\psi} \\ 1 & 0 \end{pmatrix}\begin{pmatrix} \psi_e \\ z_\psi \end{pmatrix} + \begin{pmatrix} 1 \\ 0 \end{pmatrix} d_\psi, \qquad \begin{matrix} \psi_e(0) = \psi_{e_0} \\ z_\psi(0) = 0 \end{matrix}$$

1. *Lateral/Directional Channel*

Recall the form of the closed-loop system description

$$\dot{e} = Ae + Bv$$

where A is the closed-loop linear dynamics matrix

$$\begin{bmatrix} A + BK_P & BK_I \\ I & 0 \end{bmatrix}$$

For this channel,

$$A = 0, \qquad B = [-1, 1], \qquad v = \begin{pmatrix} \phi \\ \beta \end{pmatrix}$$

$$K_P = \begin{bmatrix} K_{\phi,\psi} \\ K_{\beta,\psi} \end{bmatrix}, \qquad K_I = \begin{bmatrix} K_{\phi,z} \\ K_{\beta,z} \end{bmatrix}$$

Thus, the closed-loop linear dynamics matrix is

$$\begin{bmatrix} A + BK_P & BK_I \\ I & 0 \end{bmatrix} = \begin{bmatrix} -K_{\phi,\psi} + K_{\beta,\psi} & -K_{\phi,z} + K_{\beta,z} \\ 1 & 0 \end{bmatrix}$$

and the characteristic equation is

$$\lambda^2 + (K_{\phi,\psi} - K_{\beta,\psi})\lambda + K_{\phi,z} - K_{\beta,z} = 0$$

We want

$$\omega_{n_L}^2 = K_{\phi,z} - K_{\beta,z}, \qquad 2\xi_L\omega_{n_L} = K_{\phi,\psi} - K_{\beta,\psi}$$

Choosing, as before,

$$K_{\phi,\psi} - K_{\beta,\psi} = 1/\tau$$

and

$$\xi_L = \sqrt{2}/2$$

$\rightarrow$

$$\omega_{n_L} = 1/\left(\sqrt{2}\cdot\tau\right)$$

Choosing the same time constant as was selected in the earlier proportional case would allow the proportional and the integral parts

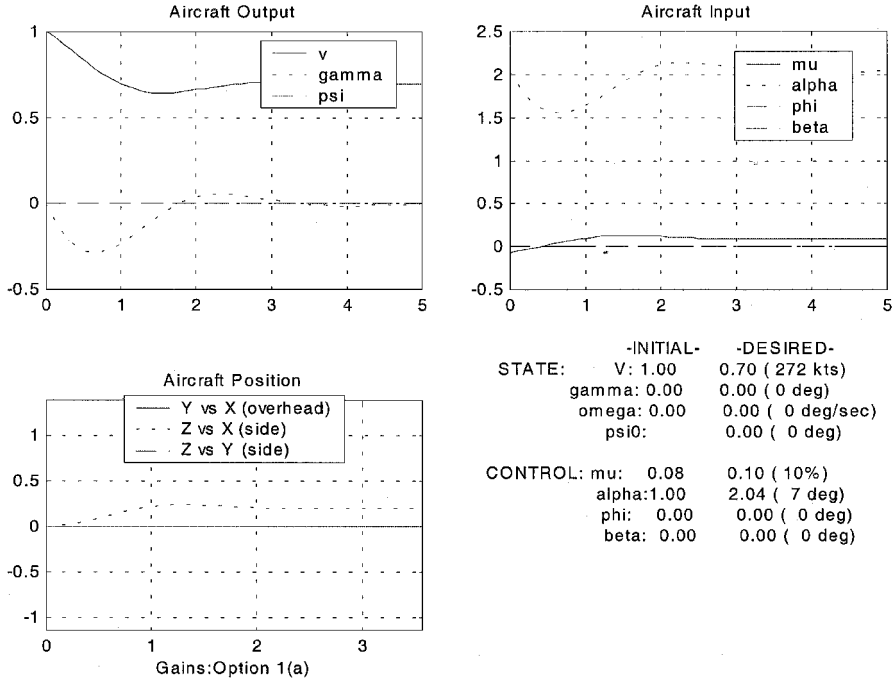

Fig. 5 Decrease speed to 0.7.

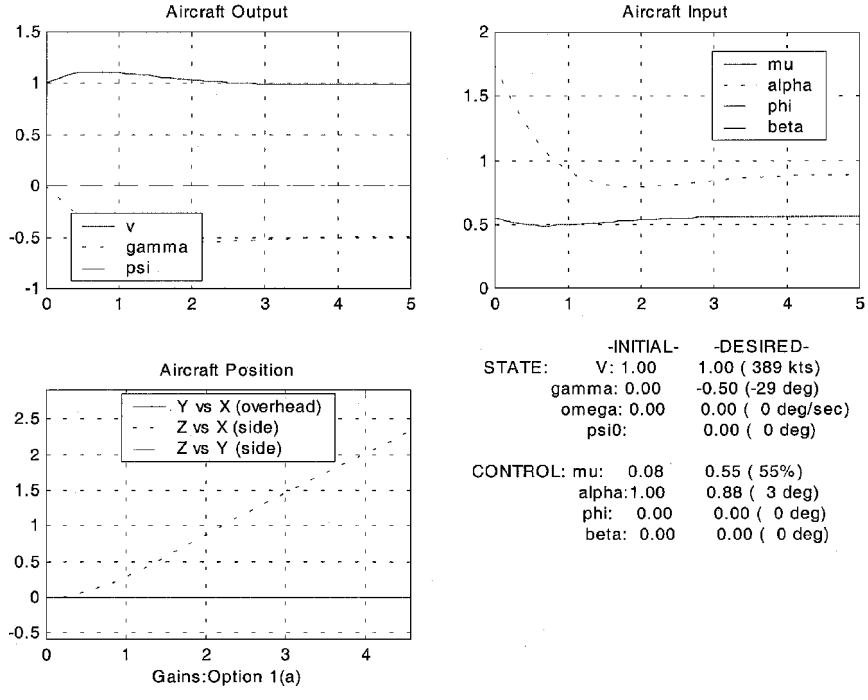

Fig. 6 Climb of 57 deg.

of the controller to track similar dynamic reference signals. Therefore, choosing $\tau = \frac{1}{2}$, as before, yields

$$\omega_{n_L} = \sqrt{2}$$

Hence, the integral action gains satisfy the equation

$$K_{\phi,z} - K_{\beta,z} = 2 \tag{15}$$

If a BTT control strategy is employed, implying $K_{\beta,\psi} = K_{\beta,z} = 0$, this defines $K_{\phi,z}$:

$$K_{\beta,\psi} = K_{\beta,z} = 0, \qquad K_{\phi,\psi} = K_{\phi,z} = 2 \tag{16}$$

If an STT control strategy is employed, implying $K_{\phi,\psi} = K_{\phi,z} = 0$, this defines $K_{\beta,z}$:

$$K_{\phi,\psi} = K_{\phi,z} = 0, \qquad K_{\beta,\psi} = K_{\beta,z} = -2 \tag{17}$$

If a hybrid BTT/STT control strategy is used, we could somewhat arbitrarily choose, for example,

$$K_{\phi,\psi} = K_{\phi,z} = 1.5, \qquad K_{\beta,\psi} = K_{\beta,z} = -0.5$$

to weight bank angle twice as heavily as sideslip angle in the controller.

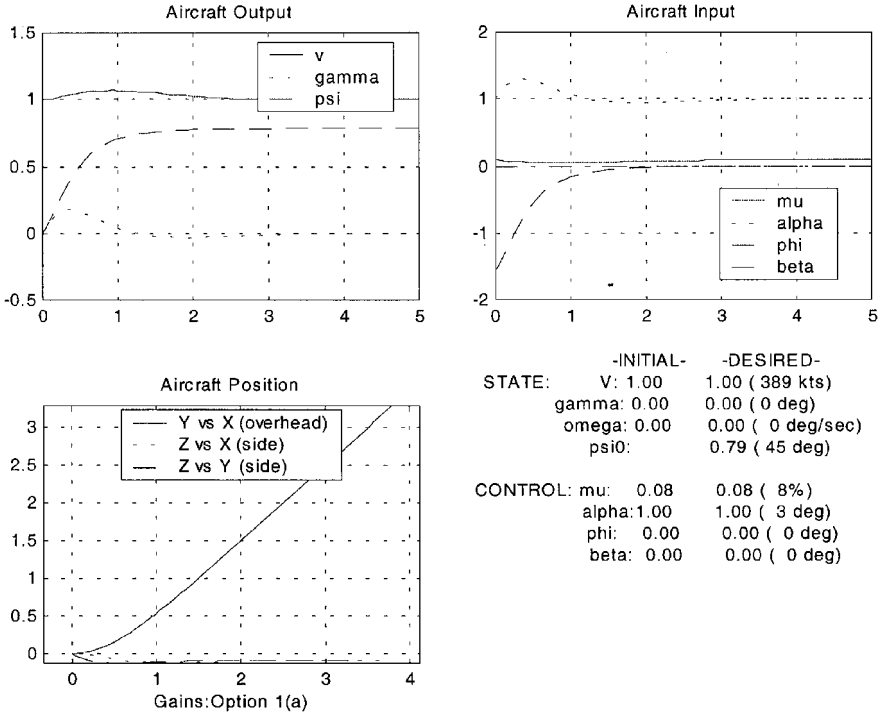

Fig. 7 Heading change of 45 deg.

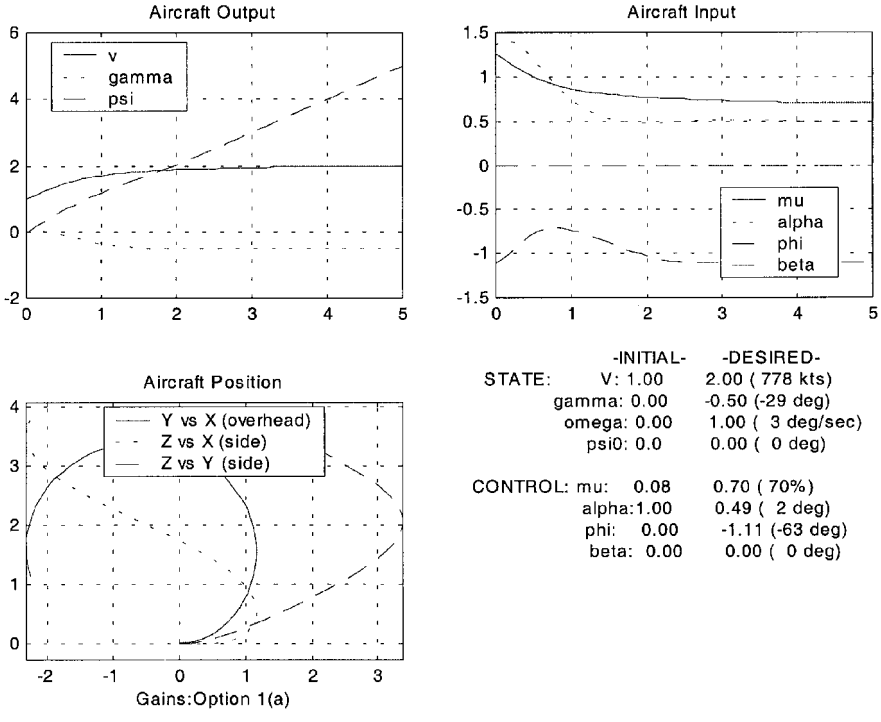

Fig. 8 Accelerate, climb, and turn.

2. Summary

When integral action is used in the lateral/directional channel, the complete control law is augmented as follows:

$$\phi = A\sin\left\{\frac{\bar{V}^2}{1+\bar{\omega}^2\bar{V}^2}\frac{1}{\cos\bar{\gamma}}\left[\bar{\omega}\bar{V}\sqrt{\frac{1+\bar{\omega}^2\bar{V}^2}{\bar{V}^4}\cos^2\bar{\gamma} - K^2_{\bar{\beta},\bar{\omega}}\bar{\omega}^2} - K_{\bar{\beta},\bar{\omega}}\bar{\omega}\right]\right\} - K_{\phi,\psi}\cdot e_\psi - K_{\phi,z_\psi}\cdot z_\psi$$

$$\beta = -K_{\bar{\beta},\bar{\omega}}\cdot\bar{\omega} - K_{\beta,\psi}e_\psi - K_{\beta,z_\psi}\cdot z_\psi$$

IV. Simulation Results

The controller is first exercised with set point commands, the specifics of which are described in Figs. 5–10. The objective is to establish the operational envelope of the controller. In addition, the controller is exercised with dynamic reference signals, demonstrating phugoid damping control. For all simulations, the initial reference signal $(\bar{V}, \bar{\gamma}, \bar{\omega}) = (1, 0, 0)$, whereas the set point commands are intended to force the initial states toward desired states.

The simulation results are summarized in Figs. 5–10. A series of maneuvers types are simulated with the intent of examining the controller's performance at the boundary of its operational envelope. High-amplitude set point changes in velocity, flight-path angle, and

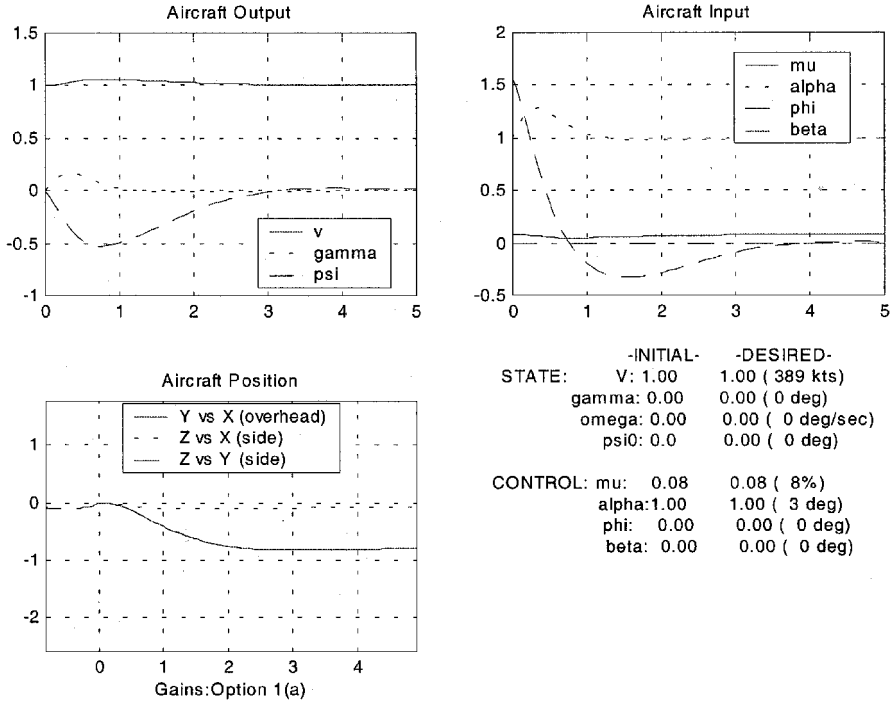

Fig. 9 Roll disturbance = $\pi/2$.

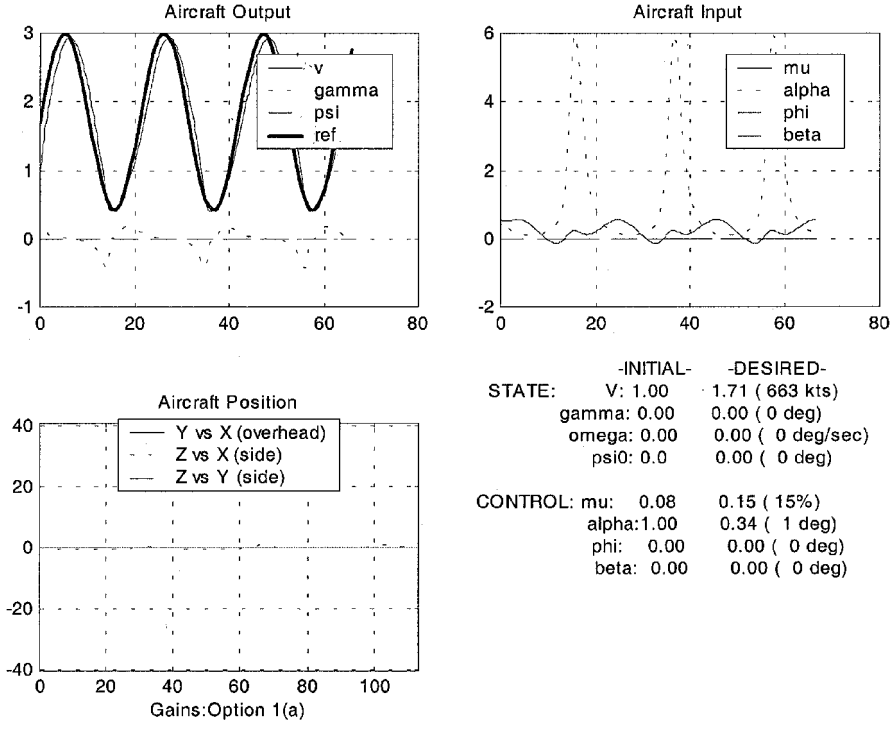

Fig. 10 Tracking of dynamic V reference = 1.7 + sin(0.3t).

heading angle are simulated, followed by a multivariable set point change, namely, maneuvers that entail simultaneous changes in the reference signals for all three states.

The controller's robustness and roll disturbance rejection performance is examined. Finally, the FCS's ability to track a sufficiently slow dynamic reference input is validated.

Figure 5 shows the FCS's response when the reference signal $\bar{V}$ is changed to 0.7. The new trim thrust $\bar{\mu}$ (0.10) is higher than the old one (0.08), and the new trim $\bar{\alpha}$ increases to 2.04. As expected, the aircraft reacts to the new reference by decreasing thrust until the new trim $\bar{V}$ is reached. As the control system applies the new trim $\bar{\alpha}$ to the aircraft still flying at the old $\bar{V}$, the flight-path angle γ increases. The compensator reacts by temporarily decreasing α until the velocity state reaches equilibrium. The trim thrust $\bar{\mu}$ increases because, in the new trim condition, the aircraft flies behind the power curve. Figure 6 shows the FCS's response to a commanded climb of $\bar{\gamma} = -0.5$. The system performs the climb maneuver without difficulty.

In Fig. 7, the desired heading is set to 45 deg. The aircraft initially rolls left, then levels out. The roll produces fluctuations in the lift vector, which perturb the longitudinal modes.

In Fig. 8, a multivariable set point change maneuver is demonstrated. The aircraft accelerates, establishes a steady climb, and enters a turning maneuver. In Fig. 9, a high-amplitude roll disturbance rejection maneuver is illustrated, thus demonstrating the robustness of the controller.

Finally, in Fig. 10, the tight tracking of a high-amplitude and dynamic airspeed command $\bar{V} = 1.7 + \sin(0.3t)$ is illustrated. The dimensional frequency of the command signal is 0.0147. The simulation results show that high-amplitude and dynamic set point changes are well handled by the phugoid damping controller. In addition, extensive simulation experiments are included in Ref. 10.

V. Conclusions

A novel phugoid damping control design methodology is developed, based on the use of wind axes and a point-mass aircraft model. A multivariable set point controller is designed which consists of the following: First, it consists of a trim calculation-based nonlinear feedforward control computer; thus, given a commanded new trim state (air speed, flight-path angle, and yaw rate), the required trim thrust setting and trim angle of attack, roll angle, and sideslip angle inputs are solved for. Second, the controller consists of a small-signal linear feedback regulator; the equations of motion linearized about the trim condition of wings level, constant altitude flight, which simplifies the dynamics to allow separation between the lateral and longitudinal control channels, are used, and a small-signal linear multivariable regulator is designed. The linear compensator also entails integral action. Thus, the controller consists of a strongly nonlinear feedforward module and a linear small-signal compensator. The novel proposed multivariable set point controller encompasses full three-axes autopilot functions. The command signals are airspeed, flight-path angle, and heading angle or heading rate. Moreover, this controller is used as a tracking controller, also known as a phugoid damping controller, provided that the bandwidth of the command signal is substantially less than the bandwidth of the closed-loop FCS.

The phugoid damping controller's performance was examined in extensive simulations, and its wide operational envelope is demonstrated. The simulations were performed using MATLAB® Simulink, with the aircraft going through a variety of multivariable, high-amplitude, and dynamic maneuvers. It is shown that the controller can accept high-amplitude commands. Thus, the air speed can be commanded to change between $\bar{V} = 0.41$ and 3.0, the flight-path angle can be varied anywhere in the full range of $\bar{\gamma} = \pm\pi/2$, and heading changes of ± 74 deg can be commanded. Heading rate commands are limited only by the maximum turn rate of the aircraft. Moreover, multivariable set point changes are also well handled by the controller. Finally, its ability to track a dynamic reference signal, as in phugoid damping control, was tested. Even with the reference signals having high amplitudes and relatively high frequencies, the control system performed successfully, as long as the (nondimensional) velocity reference signal's frequencies was below 0.57 (=0.0279 Hz). In conclusion, tight tracking of multivariable high-amplitude dynamic reference signals is possible, thus demonstrating phugoid damping control.

References

[1] Blakelock, J. H., *Automatic Control of Aircraft and Missiles*, Wiley, New York, 1991, pp. 56–182.

[2] Franklin, G. F., Powell, J. D., and Workman, M. L., *Digital Control of Dynamic Systems*, Addison Wesley Longman, New York, 1990, pp. 62–111, 143–190.

[3] Chetwyn, K., RAF Page [online journal] URL:http://www.stable.demon.co.uk/raf.htm [cited 31 Jan. 2001].

[4] van Dolderen, D. J., *The History of the RNLAF* [online journal] URL:http://web.inter.nl.net/hcc/D.vanDolderen/wo2.htm [cited 31 Jan. 2001].

[5] Garrison, P., "Aftermath," *Flying*, Oct. 1986, pp. 22–24.

[6] *Lateral vs. Directional Control Authority*, Airline Pilots Association [online journal] URL:http://safety.alpa.org/submissions/lateral.htm [cited 31 Jan. 2001].

[7] Pachter, M., Chandler, P., and Smith, L., "Maneuvering Flight Control," *Journal of Guidance, Control, and Dynamics*, Vol. 21, No. 3, 1998, pp. 368–374.

[8] Hall, J. K., and Pachter, M., "Formation Maneuvers in Three Dimensions," AIAA Paper 2000-4372, Aug. 2000.

[9] Pachter, M., D'Azzo, J. J., and Veth, M., "Proportional and Integral Control of Nonlinear Systems," *International Journal of Control*, Vol. 64, No. 4, 1996, pp. 679–692.

[10] Schindeler, N. J., "Phugoid Damping Control," M.S Thesis, Dept. of Electrical and Computer Engineering, Air Force Inst. of Technology, Wright–Patterson AFB, OH, March 2001.